MEMORANDUM REPORT BRL-MR-3992

BRL

AN EXPERIMENTAL FACILITY FOR PACKED AND FLUIDIZED BED STUDIES

CSABA K. ZOLTANI

JULY 1992

U.S. ARMY LABORATORY COMMAND

BALLISTIC RESEARCH LABORATORY
ABERDEEN PROVING GROUND, MARYLAND

NOTICES

Destroy this report when it is no longer needed. DO NOT return it to the originator.

Additional copies of this report may be obtained from the National Technical Information Service, U.S. Department of Commerce, 5285 Port Royal Road, Springfield, VA 22161.

The findings of this report are not to be construed as an official Department of the Army position, unless so designated by other authorized documents.

The use of trade names or manufacturers' names in this report does not constitute indorsement of any commercial product.

REPORT DOCUMENTATION PAGE

Form Approved
OMB No. 0704-0188

1. AGENCY USE ONLY (Leave blank)	2. REPORT DATE	3. REPORT TYPE AND DATES COVERED
	July 1992	Final, Jun 91 – Feb 92

4. TITLE AND SUBTITLE
An Experimental Facility for Packed and Fluidized Bed Studies

5. FUNDING NUMBERS
PR: 1L161102AH43

6. AUTHOR(S)
C. K. Zoltani

7. PERFORMING ORGANIZATION NAME(S) AND ADDRESS(ES)

8. PERFORMING ORGANIZATION REPORT NUMBER

9. SPONSORING / MONITORING AGENCY NAME(S) AND ADDRESS(ES)
U.S. Army Ballistic Research Laboratory
ATTN: SLCBR-DD-T
Aberdeen Proving Ground, MD 21005-5066

10. SPONSORING / MONITORING AGENCY REPORT NUMBER
BRL-MR-3992

11. SUPPLEMENTARY NOTES

12a. DISTRIBUTION / AVAILABILITY STATEMENT
Approved for public release; distribution is unlimited.

12b. DISTRIBUTION CODE

13. ABSTRACT (Maximum 200 words)

The design of an experimental facility for the study of drag resistance in stationary and fluidized gun propellant beds is described. It establishes the capability for the simulation of flows at five times the Reynolds number and in tubes of four times the cross-sectional area heretofore reported. The design makes possible for the first time, at Reynolds numbers encountered in a ballistic packed bed, unlimited running times. In addition, transient flow conditions can also be simulated.

14. SUBJECT TERMS
fluidized bed processes, ballistics, packed beds, flow measurement, Reynolds number

15. NUMBER OF PAGES
36

16. PRICE CODE

17. SECURITY CLASSIFICATION OF REPORT	18. SECURITY CLASSIFICATION OF THIS PAGE	19. SECURITY CLASSIFICATION OF ABSTRACT	20. LIMITATION OF ABSTRACT
UNCLASSIFIED	UNCLASSIFIED	UNCLASSIFIED	SAR

INTENTIONALLY LEFT BLANK.

TABLE OF CONTENTS

INTENTIONALLY LEFT BLANK.

LIST OF FIGURES

LIST OF TABLES

INTENTIONALLY LEFT BLANK.

ACKNOWLEDGMENTS

It is a pleasure to thank Mr. Fred Robbins, Ballistic Research Laboratory (BRL), for sharing his experience related to fixed bed resistance experiments. Thanks are also due to Ms. Liz Marcou, BRL, for drawing the figures.

INTENTIONALLY LEFT BLANK.

1. INTRODUCTION

Gun performance predictions rely on the availability of packed and fluidized bed drag data. Due to the difficulty and cost, only a very limited amount of exoerimental bed drag data is available at the present time. To fill this gap, a new flow rig, which allows routine data generation under a wide variety of conditions, was designed.

The resistance to flow through packed beds has many industrial applications and has received wide attention. Some of its relevance to the ballistic problem has been summarized recently in Zoltani (1991). Industrial interest usually centers on low velocity flows and, therefore, the experimental results must be interpreted with caution when used in a ballistic context. Current practice has its antecedents in the research of Forchheimer (1901) and Ergun (1952) and is basically an attempt to record pressures on the walls of the container of the packed bed. Cold flow experiments of interest to ballisticians have been reported by Jones and Krier (1983), Wilcox and Krier (1980), Kuo and Nydegger (1978) and Robbins and Gough (1978) (see Zoltani [1991, Tables 1 and 2]).

Table 1. Packed Bed Simulators

Reference	Bed Diameter (cm)	Test Section Length (cm)	Particle Scale (cm)	D/d_p	p_{max} (MPa)	Remark
Ergun (1952)	2.54	20.0	0.02–0.10	25–111	—	glass, lead shot
Kuo et al. (1978)	0.77	30.0	0.0826	9.3	14.0	WC 870 ball
Robbins et al. (1978)	7.62	93.0	1.39–30.3	9.6–60	20.0	perf
Jones et al. (1983)	2.54–5.08	20.3	0.96–6.0	8.5–50	2.5	glass beads
proposed work	15.24	100.0	1 cm up	15	7.0	—

Table 2. Drag Correlations in Use

Reference	Coefficient of Drag, Fv	Shape	Reynolds No./Void Regime
Ergun (1952)	$F_v = 150 + 1.75\,\hat{Re}$	various	$0.67 < \hat{Re} < 2300$ $0.4 < \varepsilon < 0.65$
Kuo & Nydegger (1978)	$F_v = 276.23 + 5.05(\hat{Re})^{0.87}$	spheres	$767 < \hat{Re} < 24\,330$ $0.37 < \varepsilon < 0.39$
Robbins & Gough (1978)	$F = 2.5\,\hat{Re}^{-0.081}\lambda^{2.17}$	spheres cylinders	$\hat{Re} < 121\,675$ $0.396 < \varepsilon < 0.509$
Jones & Krier (1983)	$F_v = 150 + 3.89(\hat{Re})^{0.87}$	spheres	$737 < \hat{Re} < 126\,670$ $0.38 < \varepsilon < 0.44$

Note: Here $\hat{Re}$ is the Reynolds number divided by $(1 - \varepsilon)$. Note that the correlation of Robbins and Gough is the inverse of F_v, i.e., defined as

$$F = \frac{\Delta p}{L}\,\frac{d_p \rho}{(\rho U)^2}\,\frac{\varepsilon^3}{1-\varepsilon},$$

where the symbols are the same as defined for Equation 1. For details see Jones and Krier (1983). λ in Robbins and Gough is a shape factor.

In these experiments, the flow was assumed to be steady and much of the data was taken at moderate to low Reynolds numbers. The flow medium being bottled gas, the time available for the acquisition of data was limited. This fact also precluded the determination of velocity profiles. The measurements were used to establish correlations between Reynolds number $\hat{Re}$, where the Reynolds number used has been divided by the $1 - \varepsilon$, and friction factor for beds of given porosity, see Table 2. There, F_v, in the formulation of Ergun (1952), is the friction factor. In other words,

$$F_v = \frac{\Delta p}{L}\,\frac{d_p^2}{\mu U}\,\frac{\varepsilon^3}{(1-\varepsilon)^2}, \qquad (1)$$

where Δp is the pressure drop, d_p the particle diameter, ε the void fraction μ the gas viscosity, and U the velocity is as defined in Equation 3, and L the bed length. Values of F_v increase with increasing $\frac{Re}{1-\varepsilon}$ from 150 into the thousands. The total energy loss in the bed is the sum of both viscous and kinetic energy losses, but depending on the Re number regime, one or the other may predominate. These

correlations rely to various degrees on Ergun's (1952) results. The effect of the proximity of the walls is not directly included. Validity of the correlations are restricted to the indicated Re number and porosity regimes. Extrapolation of the formulas to outside these regimes usually entails a serious error. A number of unanswered questions remain, including: Are radial pressure gradients present in the bed? and What is the nature of the velocity field in and past the bed?

The next sections describe the requirements on the experimental facility followed by the actual specifications required to attain these goals.

2. REQUIREMENTS ON THE NEW TEST FACILITY

To extend the existing database on packed bed propellant drag, an experimental rig was designed to generate flows with Reynolds numbers, based on propellant length scale of 1 cm, to exceed 10^5 in the test section. Beds up to 155 mm in diameter need to be accommodated.

The experiments must yield the following data:

(1) gas mass flow rate
(2) pressure at several stations along the packed bed
(3) temperature at the entrance and exit of the bed
(4) velocity profiles of the gas flow at the entrance and the exit of the bed
(5) boundary layer profiles in the presence of ullage and in the two-phase medium

Propellants of different shapes, sizes and perforations at different densities of loading will constitute the bed components. Means of restraining the bed from moving during the experiment must be devised.

The measurement of velocity profiles in tubes, especially near curved wall surfaces, is a challenging task. For an adequate resolution of the boundary layer and flow profile in each of the two perpendicular coordinate directions at each cross section requires between 15 and 20 data points per radius. The symmetry of the flow is checked by taking data across the whole cross section. The data taken at each and every location must be repeatable within a small percentage of deviation. Prudent experimental practice requires that data be checked repeatedly and often to find errors in the flow or the

instrumentation. The bottom line is that at the upstream and downstream locations where velocity assays are required, in excess of 240 measurements each may be required for a total of around 500 measurements.

To date, propellant bed drag experiments were run with bottled gas. However, velocity measurements impose a taxing burden on the gas supply. To illustrate, for a given propellant bed, to take 500 velocity measurements, the flow taking place at Re = 10^5 would require the following quantities of gas: a size 300 gas cylinder of 1.75 ft^3 capacity (49.6 liters), say, initially at 2,490 psi (1.71×10^7 Pa) and a throat area of 1.24×10^{-5} m^2 (piping of 5/32-inch ID) empties in about 174 seconds when the flow is choked. (For an overview of the blowdown process see the Appendix.) In a reasonably seeded flow, the acquisition of data by LDA takes about 10 seconds per point. The traversing table must then be moved to the new position, which takes another 10 seconds at the minimum. Thus, allowing for a 10% wastage, eight data points per gas cylinder can be anticipated. One can then conclude that 62 bottles of gas at $90 each for ultra high purity nitrogen (since it must be oil free), or about $6,000 per experiment in gas cost alone can be anticipated. This may be somewhat optimistic since many times, due to uneven seeding and other factors related to the nature of Laser Doppler Anemometry (LDA) data acquisition, more time per data point may be logged. To shut off the gas supply between data positions is not practical since flow transients will be introduced and time must be allotted for these to die down. One sees then that using bottled gas is not an economical way to proceed. An alternative way of supplying the required amounts of gas is needed and is suggested below.

3. DESIGN OF THE FLOW RIG

3.1 Background. Drag, or resistance to flow, can be inferred from the pressure drop caused by the presence of the obstacle in the flow. Differential pressure flow metering devices such as orifices, sonic nozzles, and venturis rely on the fact that the pressure distribution in a flow can be related to the flow rate. Thus, if the pressure drop caused by the presence of a device can be accurately recorded, a direct relationship to the flow rate can be established. Accelerating the flow through a constriction of known area and knowing the resulting pressure drop, the mass flow rate can be determined.

Three coefficients are of interest: the flow coefficient, C_d ; the discharge coefficient, C_D ; and the pressure drop coefficient, K. Recall that the pressure drop between two axial stations, x_1 and x_2 in a tube under incompressible flow assumptions, is directly proportional to the distance $x_2 - x_1$.

$$\Delta p/(0.5\rho U^2) = f(x_2 - x_1, \frac{1}{D}, Re) \tag{2}$$

where U is the mean approach flow velocity, D the tube diameter, ρ the gas density, and the right side is a functional relationship. We note that the Fanning factor, more commonly used in aerodynamics, is one-quarter as large as f. A relationship for f can be obtained by combining the continuity equation

$$m = \rho Q = \rho A U \ , \tag{3}$$

with Equation 2,

$$\frac{1}{f} = \frac{\rho^2 U^2 A^2}{2\rho \Delta p A^2} . \tag{4}$$

Taking the square root of both sides and defining $\hat{f} = \sqrt{\frac{1}{f}}$, one gets

$$\hat{f} = m/[A\,(2\rho\Delta p)^{0.5}] \ . \tag{5}$$

Also, it should be noted that measurement accuracy is increased when Δp is large. Since the flow rate Q is proportional to the square root of the pressure drop (i.e., if the variation in p is 10 to 1), the corresponding flow rate variation is 3 to 1. This can be easily inferred from $m = \rho Q = f\Delta\sqrt{2\rho\Delta p}$, i.e., $Q \sim \sqrt{\Delta p}$.

For a flow meter, the friction factor is commonly referred to as a flow coefficient C_d and expressed as

$$C_d = \frac{Q}{A_2}\left(\frac{\rho}{2\Delta p}\right)^{0.5} = \zeta\ (\lambda,\ k/D,\ Re) \ , \tag{6}$$

where Q is the volume flow rate, λ is the area ratio $\left(\frac{A_2}{A_1}\right)$ of the orifice to the pipe cross-sectional area A_1, k is the roughness of the pipe, the pipe diameter is D, and Re is the Reynolds number. Note that $C_d = f$.

Recalling that the pressure difference upstream of the constriction to that at the minimum cross-sectional area of the flow can be related to the area ratio as

$$\Delta p \sim (1 - \lambda^2) , \tag{7}$$

the effect of the magnitude of the area ratio on the magnitude of C_d can be reduced by dividing Δp by $(1 - \lambda^2)$, yielding the so-called discharge coefficient, C_D.

$$C_D = (Q/A)/\left[\rho (1 - \lambda^2)/(2\Delta p)\right]^{0.5} . \tag{8}$$

C_D is the true flow rate divided by the theoretical flow rate and the relationship between C_d and C_D is given by

$$C_D = C_d(1 - \lambda^2)^{0.5} . \tag{9}$$

At higher Reynolds numbers the discharge coefficient can be expressed with an equation of the form

$$C_D = C_\infty + b/Re^n , \tag{10}$$

where the C_∞ is the discharge coefficient at infinite Reynolds number, and b and n are constants (Miller 1989). Typically, at $Re = 10^5$, the discharge coefficient is around 0.6. Finally, the pressure drop coefficient is defined as

$$K \equiv \Delta p/(0.5\rho U^2) = \left[(1 - \phi\lambda)/(\phi\lambda)\right]^2 , \tag{11}$$

where ϕ is the coefficient of contraction A_v/A_2; A_v is the area of the vena contracta, the smallest area of the discharge past the orifice plate; A_2 is the orifice cross-sectional area; and λ, as before, is an area ratio.

The right-hand side of Equation 11 follows from straightforward manipulation of the conservation laws for incompressible flow.

3.2 Specification of the Components. An overview of the flow rig is given in Figure 1. One of the innovations introduced is that the rig incorporates its own gas source, furnishing air at a rate high enough to ensure that the desired Reynolds number in the test section is reached. Upon leaving the compressor, the gas enters the test section after traversing a flow straightener (ASME-type, perforated, multiplate flow rectifier). The gases exiting the test bed go through a second flow straightener and the sonic nozzle metering section before exiting. By carefully calibrating the sonic nozzle, it may be adapted to function as a metering device both in the choked and subsonic regimes, alleviating the need for an orifice plate for flow measurement when subsonic conditions prevail. Pressure probes across the flow meters, along the test section as well as temperature gages fore and aft of the test bed will be mounted as shown in Figure 1. Optical access to the flow will also be provided to enable velocity measurements to be made by state-of-the-art flow diagnostic techniques (Figures 2 and 3), see for example Dybbs and Ghorashi (1991).

The sonic nozzle flow meter assembly of Smith-Matz geometry with a 1.798-inch (0.045-m) throat, contains the flow rectifier, inlet temperature, inlet pressure, and throat taps with a balancing manifold. Sonic and subsonic calibration need to be provided with the unchoking test. It is felt that the discharge coefficient variation can be held to be within 0.5%. The associated instrument package includes the inlet temperature, pressure and differential pressure probes, and transmitters. The data acquisition board for a 286-type computer and custom software will display the mass, volumetric flow rates, and the status and readings of the pressure probes.

The modus operandi adopted here was to start at the back of the rig (exhaust end), calculate the pressure drop through each of the components, and thus arrive at the performance required of the device furnishing the required amount of air. The calculations were based on a standard 6-inch (152.4-mm) pipe, which, due to cost considerations, is preferable to a specially fabricated 155-mm tube.

3.2.1 Straight Pipe Section. The pressure drop in a pipe under steady flow conditions, as already shown in Equation 2, is given by the following relationship,

$$\Delta p = f(L/D)\rho U^2/2 \ , \qquad (12)$$

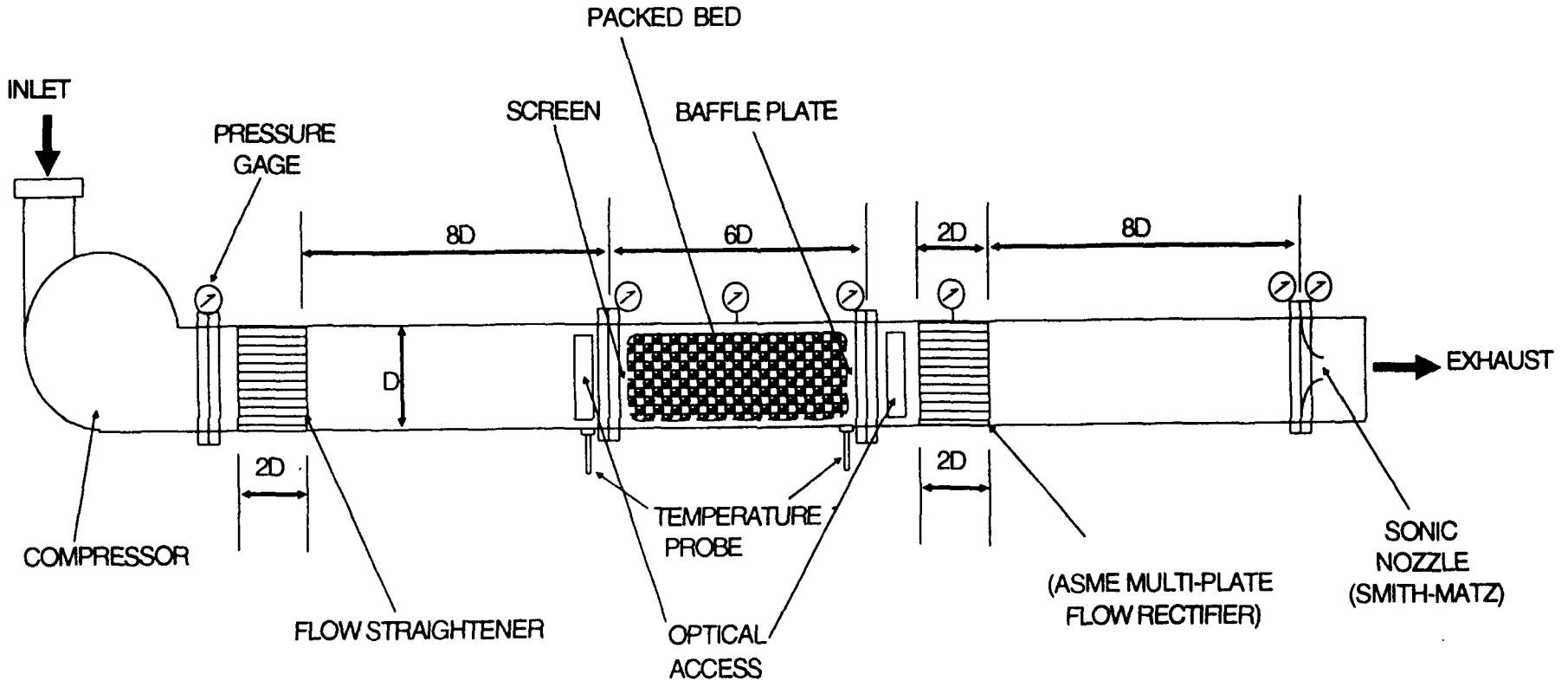

Figure 1. Side View of Flow Rig for Fixed Bed Studies.

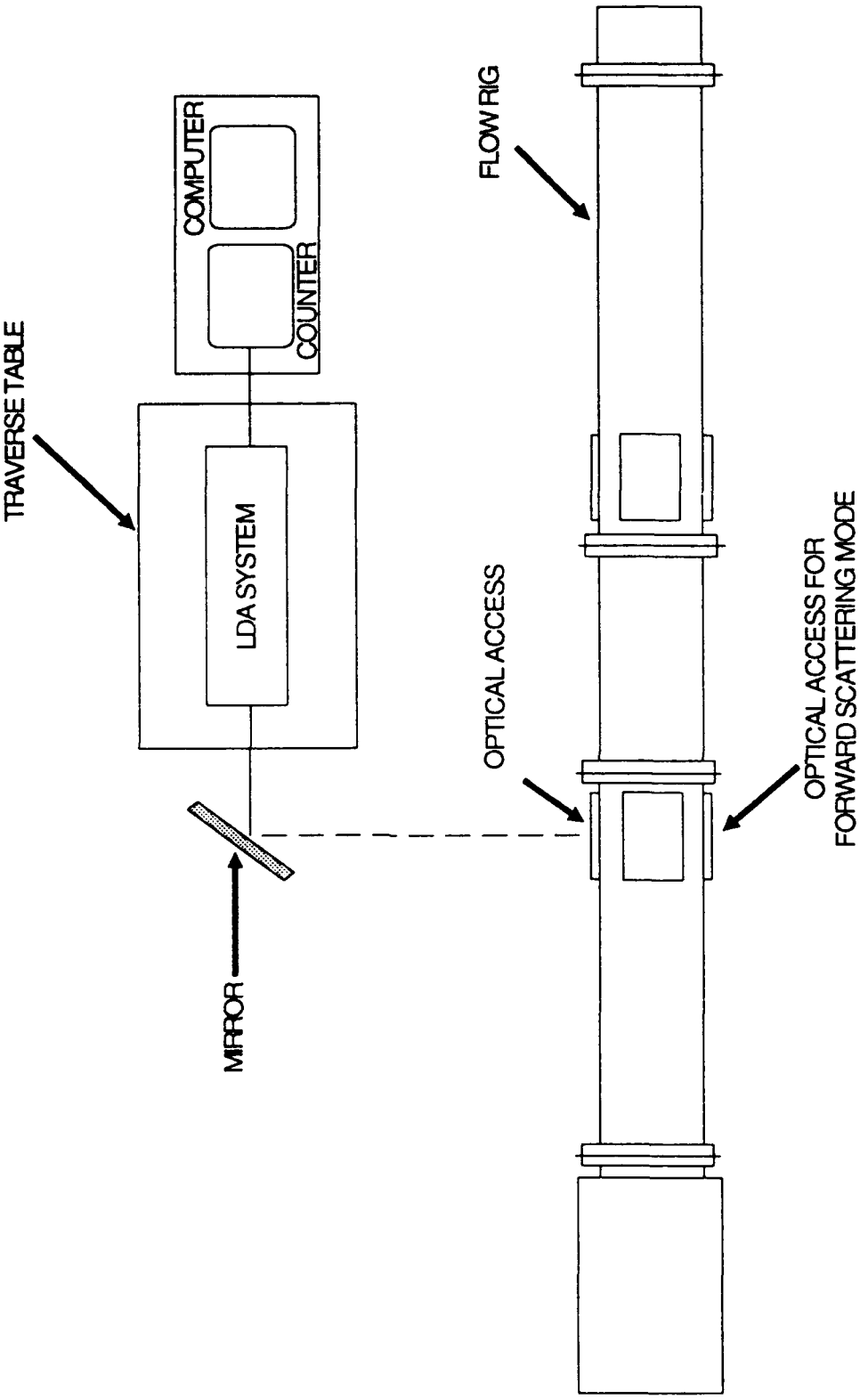

Figure 2. Instrumentation for Laser Doppler Anemometry (LDA) Velocity Field Analysis (Top View).

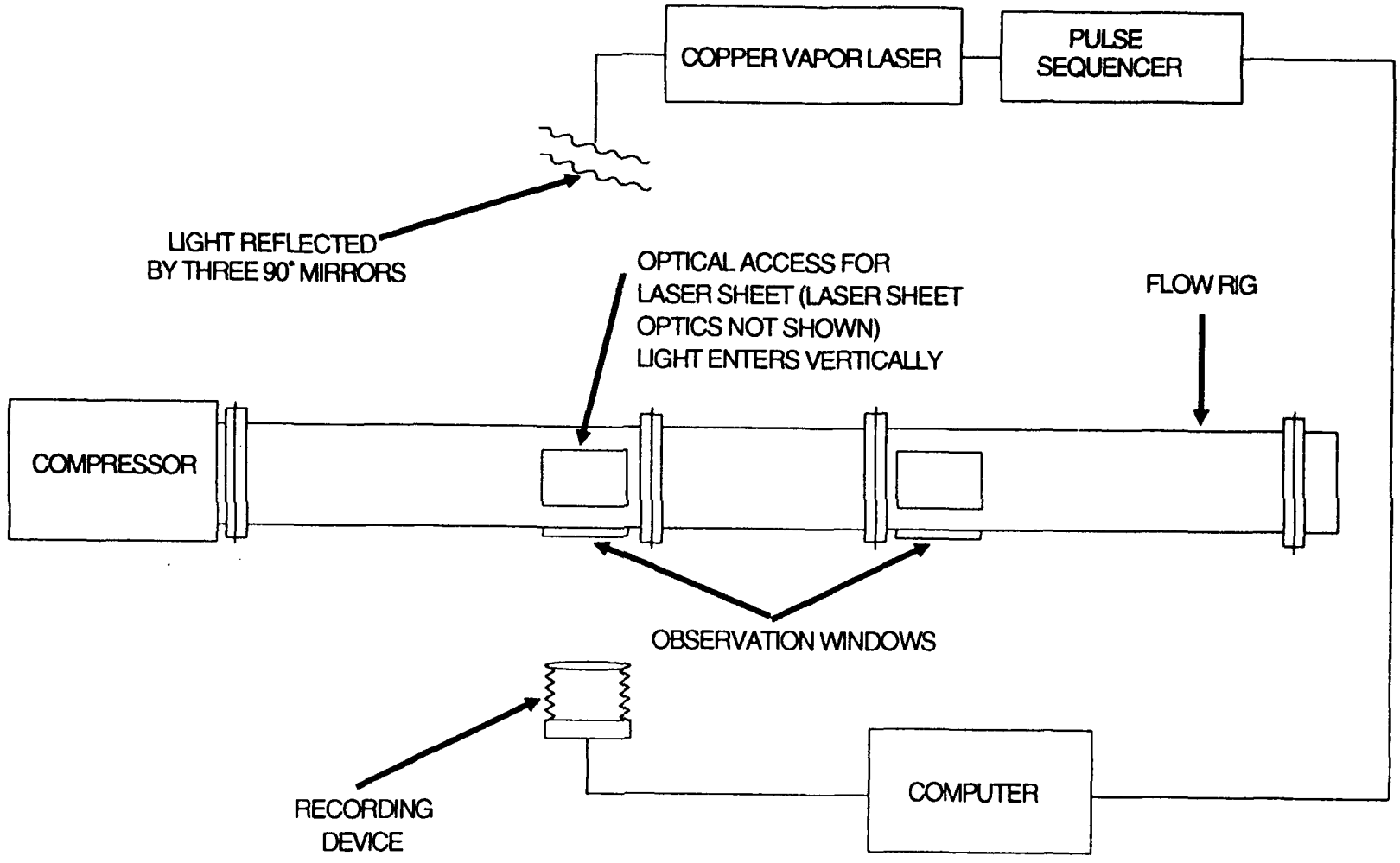

Figure 3. Particle Image Velocimetry (PIV) Diagnostics for Velocity Mesurements (Top View).

where, as usual, f is the friction factor, L the length of the pipe section, D the diameter, and ρ the density of the fluid. Machining costs dictate that pipe sections should not exceed 1 meter in length. Commercially available steel pipes have an f value of around 0.02 at Re = 10^5. Thus, the pressure loss in a 1-meter pipe section, under the conditions of interest here (ρ = 1.2 kg/m^3, U of the order of 10 m/s, and L/D = 6) will be 185 Pa and the K value is 0.12 based on

$$K = f \cdot L/D = \Delta p/(0.5\rho U^2) \ . \tag{13}$$

3.2.2 Loss at an Orifice. For a Class 2 orifice (i.e., one having sharp edges and made of thin plate) and $t < 0.1d$ where d is the orifice opening diameter, t the orifice material thickness, and Re > 10^3, where the Re number is based on the orifice diameter, in the nomenclature of Ward-Smith (1980), and noting the similarity to Equation 10, i.e., $\xi = \lambda$,

$$K = \left[(1 - \phi\xi)/(\phi\xi)\right]^2 \ . \tag{14}$$

Here ξ is the orifice opening to the tube area ratio and ϕ the contraction ratio. Ward-Smith (1980) gives tabulations of ϕ vs. ξ. For ξ = 0.5, K turns out to be 4.954. Equation 14 is derived by using the definitions of ϕ, ξ in conjunction with the incompressible conservation equations between the upstream, vena contracta and downstream positions of a metering device.

3.2.3 Flow Straightener. The accuracy of flow metering devices depends on whether the flow is fully developed and on the success of eliminating transverse motion (i.e., swirl) in the flow. Several studies exist on the effect of swirl on the discharge coefficient of an orifice plate (Zanker 1962). Kinghorn (1977) determined discharge coefficient bias errors for venturis and orifices. For a swirl angle of fifteen degrees, typically, the error can approach 10%. BSI (1963) stated, as was also confirmed by Kreith and Sonju (1965) and Miller (1989), that the persistence of swirl may extend over considerable distances. Without a flow straightener, general practice suggests (Miller 1989) that 100 pipe diameters may be needed to attenuate, at Re = 10^4 a swirl at 2°. ISO Standard 5167 (1980) states that "Acceptable velocity profile conditions can be presumed to prevail when at each point across the pipe cross section the ratio of local axial velocity to the maximum axial velocity at the cross section located at the end of a very long straight length over 100 D of similar pipe." Flow straighteners remove the necessity of including long runs of straight tubing to achieve fully developed flow conditions.

Swirl has several effects on the flow: with increasing swirl, the position of the maximum axial velocity moves progressively away from the tube axis. Consequently, there is a reduction of the axial velocity along the axis and, at high enough swirl, reversed flow can occur at the pipe axis. Swirl can defined by a parameter W as follows:

$$W = 4M_{ang}/(\pi\rho U^2 D^3) , \tag{15}$$

where M_{ang} is the angular momentum flux. As shown by Baker and Sayre (1974), the ratio of the mean to fully developed flow without swirl friction factors can be given as

$$f_m/f = 1 + 11.5W^{1.32} \exp(0.45\, L/D) , \tag{16}$$

where L is the distance between measuring stations and D the pipe diameter. The relation is valid for $1.25 \times 10^4 < Re < 2.0 \times 10^5$. Lugt (1963) describes a simple device which can indicate the presence of swirl in a pipe flow. It consists of a fitting with two pressure holes side by side on the periphery of the pipe. A swirl at the wall will produce a differential pressure detectable by a simple manometer.

Thus, the basic objective is to remove major flow distortions of the axial velocity so that fully developed flow conditions exist at all metering devices. Toward these ends, a number of authors have suggested remedies, here we discuss two of them. It is important to minimize the value of K of these devices so that the pressure loss occurring there remains small. Sprenkle and Courtright (1958) proposed a three-plate arrangement with one tube diameter spacing between plates with holes amounting to about 1/2 of the pipe cross section distributed over the plate. A value of K = 16 was measured for the device. This value declined to 11 when the inlet side of the orifices was beveled. It was also found that a length of eight diameters before the orifice after the flow straightener assured settling of the flow and elimination of metering errors.

An improvement in the K value was reported by Zanker (1962) with a single perforated plate but with orifices of different sizes distributed on the plate. The largest hole was placed near the axis and a honeycomb (one pipe diameter in length) was attached to the plate. The cells were square with their axes coinciding with the holes in the plate. The settling length was four pipe diameters and the velocity profile was found to approach that of fully developed flow. At $Re = 10^5$, the K value was 5.7; while at $Re = 10^6$,

it declined to 5.1. Kinghorn et al. (1976) report a further improvement with a straightener-venturi nozzle package. The Mitsubishi conditioner (Miller 1989) is easier to fabricate than that due to Zanker, however, the design is proprietary.

3.2.4 Perforated Plates and Baffles. To hold the test bed in place, either a screen or plate and a baffle may be used. A perforated plate may be treated as an orifice plate with an opening equal to the sum of the holes in the plate.

Assume a plate of thickness t with N orifices of diameter d. The porosity of the plate ξ is defined as

$$\xi \equiv \pi N d^2/(4A) , \tag{17}$$

where A is the pipe cross section. For t/d < 0.8, Ward-Smith (1980) gives the following relation:

$$K = \left[(0.609 \xi \{1 - (t/d)^{3.5}\} \{1 - \xi^{2.6}\} + \xi^{3.6})^{-1} - 1\right]^2 , \tag{18}$$

which correlates data in the range $0.006 < \xi < 0.75$ with a root-mean-square error of 10% in the value of K. K can vary widely; indeed, Ward-Smith (1980) quotes values from 0.57 to 3.58×10^5.

3.2.5 Screens. The upstream end of the propellant bed is usually held in place by a screen. A wire mesh may be characterized by the number of wires per unit length, m (units of inverse length), and the porosity ξ, of wire strands of diameter d.

$$\xi \equiv (1 - md)^2 . \tag{19}$$

Gauzes and screens offer a high resistance to the flow compared with the wall shear stress in developing or fully developed flow. A sudden change in pressure is experienced when flow traverses the screen. Experimental values are given in both Ward-Smith (1980) and Miller (1990).

Conventionally, the flow through each aperture in a screen is viewed as the flow through a single orifice of porosity ξ. Note that Ward-Smith (1980) reports that at high Reynolds numbers, with turbulent

flow, K is independent of Reynolds number. Under these conditions, de Vahl-Davis (1964) gives the following relationship,

$$K = K_{\infty} + 55/Re = \left[(1 - \phi\xi)/\phi\xi\right]^2 + 55/Re \ . \tag{20}$$

K_{∞} is the value of K at high Reynolds. Ward-Smith (1980), for $Re > 10^3$ and $0.3 < \xi < 0.9$, gives curves of K as a function of a pressure parameter, $[(1 + K_{\infty}^{0.5})\xi]^{-1}$. Alternatively, Ower (1977) gives for the resistance of a gauze screen the expression,

$$K = 6.5[(1 - \beta)/\beta^2][Ud/\beta(\mu/\rho)]^{-1/3} \ , \tag{21}$$

where β is the open area of the gauze, U the velocity ahead of the screen, d the diameter of the wires, and (μ/ρ) the kinematic viscosity of the air. No general formula for the resistance of honeycombs is known, but some data is available from Whitaker et al. (1970) and Wieghart (1953).

3.2.6 Test Bed. The pressure drop through the test bed was calculated on the basis of Ergun's (1952) theory neglecting the first term, the constant 150, which is small with respect to the retained second term (see Table 2).

$$\Delta p/L = 1.75[(1 - \varepsilon)/\varepsilon^3]\rho U^2/d_p \ . \tag{22}$$

Here, d_p is the particle mean diameter, ε the void fraction, and ρ the gas density.

3.2.7 Sonic Nozzle. The advantage of sonic nozzles as flow measuring devices is that upstream of the nozzle changes in the downstream conditions, as long as the nozzle is choked, are not felt. The pressure recovery across the nozzle can approach 92%, however, a more conservative and likely figure is 85%. It is also possible to instrument the sonic nozzle so that it can act as an orifice plate when sonic conditions are not reached.

3.2.8 The Choice for a High Pressure Gas Source. The estimated pressure drop through the flow rig is given in Table 3. The Reynolds number at the entrance to the test section, based on a propellant particle size of 1 cm, an approach velocity of 6.41 m/s and gas density of 73.2 kg/m^3, is 2.5×10^5. The

Table 3. Pressure Loss Summary

Component	Pressure Drop (Mpa)	Comments
flow straightener	0.0077	ASME type
straight section	0.0003	steel tube
wire screen	0.0030	—
test section	4.9340	Ergun's eq.
wire screen	0.0030	—
baffle plate	0.0315	—
flow straightener	0.0003	ASME type
straight section	0.0003	—
sonic nozzle	0.2200	est. 15% loss

particle loading ε was taken to be 0.5. Allowing for a 5% pressure loss in the system due to extraneous causes, the gas must be supplied at a pressure exceeding 6.0 MPa.

As pointed out in Section 2, for a gas source, bottled gas in view of the anticipated cost is not a viable option. Rather, an situ generation of the pressurized gas suggests itself. Though the up-front investmentmay be higher than for the conventional approach, the facility will pay for itself in gas cost savings in a short period of time.

Several types of compressors (see Pichot [1986] and Compressed Air and Gas Institute [1989] for details) need to be considered. Basically, one can distinguish between positive displacement types (i.e., reciprocating, rotary, dynamic, centrifugal, and axial) and thermal types, that is injectors. Reciprocating compressors can produce gases in the tens of thousands of psig, are flexible and efficient. Their big drawback is that they require large foundations due to the unbalanced inertial forces and, most importantly, the gas flow is discontinuous. Thus, their use in the packed bed studies can only be comtemplated in conjunction with the use of a gas accumulator.

Screw-type rotary compressors are capable of handling flows ranging from 200 to 20,000 m^3/hr under discharge pressure ranging from 3 bar gage in a single stage to about 13 bar gage in two stages. These compressors use two spiral lobed rotors whose hollows are filled with gas at the inlet port. Compression begins because of the spiral configuration (i.e., during rotation the contact surfaces move parallel to the

axes of the rotors toward the outlet causing gradual compression until the trapped air is put at the outlet port).

Centrifugal compressors can reach discharge pressures of 10,000 psi (68.94 MPa) with an inlet capacity better than 200,000 acfm (94.38 m^3/s). Staging is usually employed. Ambient air is accelerated by the first impeller, then a diffuser converts the velocity into pressure. A heat exchanger cools the air before it flows through a second stage impeller and is then discharged through an aftercooler to the user. Axial machines, on the other hand, have even higher capacities but their discharge is limited to 500 psi (3.44 MPa).

3.2.9 Optical Access. Velocity measurement in the flow requires optical access. At elevated pressures, windows must be specially fabricated. With a Young's modulus of 50×10^6, modulus of rupture up to 100,000 psi (689.4 MPa), sapphire has the needed strength and optical qualities. At 0.5 μm wavelength, transmittance approaches 85% and the index of refraction is 1.77. The hydrostatic burst strength of simply supported windows is 8,300 psi (57.22 MPa). Thus, to maintain 1,000 psi (6.89 MPa) with a safety factor of four, the manufacturer, Union Carbide (1988), recommends a thickness to diameter ratio of a window of 0.15.

3.2.10 Tube Material Strength. In tubes where the radius to the tube wall thickness exceeds 10, the circumferential stress can be calculated based on the following relation (Gere and Timoshenko 1990),

$$\sigma_1 = (pr)/5 \ , \tag{23}$$

where p is the pressure inside the tube, r the radius, and t the wall thickness. The longitudinal stress follows from

$$\sigma_2 = (pr)/(2t) \ . \tag{24}$$

Taking, as a typical example, a steel tube of 0.15 m (6 inch) ID, wall thickness of 0.0063 m (0.25 inch), with a safety factor of 4, say at 13.78 MPa (2,000 psi) in the flow, the stresses are well below the allowable yield and tensile stresses of commercially available, resistance-welded carbon steel pipes of 68 and 76 ksi (4.68×10^8 Pa), respectively.

4. RESULTS

To create the desired flow conditions in the test cell, the best solution is to use a compressor. Experiments can be run indefinitely, a great advantage when performing difficult flow surveys. Unsteady flow conditions can also be simulated.

In choosing a compressor, several trade-offs must be considered. Most of the centrifugal compressors on the market guarantee high flow rates but at moderate to low pressures. The present requirement calls for high pressures by compressor standards, but at fairly low flow rates. Also, as the compressor gas exit velocity increases, due to the U^2 term (Equation 22), the pressure drop through the bed increases rapidly putting a large demand on the gas generator.

To reach the required Reynolds number at the entrance to the test section, and assuming gas exit temperatures of 300 K (which is realizable if the compressor comes with a heat exchanger), a multi-stage compressor is required. For example, the Bauer Model B 28.3 three-stage compressor discharges air at 300 K, a density of 73.20 kg/m^3, and a pressure of 6.40×10^6 Pa. At a flow rate of 250 cfm (0.117 m^3/s), the velocity is 6.41 m/s, yielding a Reynolds number of 2.5×10^5.

The facility will allow the generation of data heretofore unavailable and needed by interior ballistic modelers. By including a particle disperser and a means of recovering the propellant in the experimental rig, many aspects of the fluidized bed can also be simulated. This could include but is not limited to ullage, center core, and velocity field data in addition to detailed drag data.

5. CONCLUSIONS

A new experimental facility for the measurement of inert propellant bed drag has been designed. Its operational envelope encompasses Reynolds numbers in excess of 2.5×10^5 in test beds up to 155 mm in diameter. Both steady-state and time-dependent operations are possible. In steady state there is no restriction on the time for the experiment. This allows the taking of velocity profiles of the flow. The experiment is also instrumented with both LDA and PIV (particle image velocimetry) data acquisition systems enabling for the first time the determination of both the pressure along the test section as well as velocity profiles and turbulence data fore and aft of the packed bed.

INTENTIONALLY LEFT BLANK.

6. REFERENCES

Baker, D. W., and C. L. Sayre. "Decay of Swirling Turbulent Flow of Incompressible in Long Pipes." Proceedings of the Symposium on Flow: Its Measurement and Control in Science and Industry, vol. 1, pp. 301–12, R. B. Dowdell (ed), Instrument Society of America, 1974.

British Standards Institution. Methods of Testing Fans for General Purposes. BSI 848, Part 1, London, 1963.

de Vahl-Davis, G. "The Flow of Air Through Wire Screens." Proceedings of the First Australaian Conference on Hydraulics and Fluid Mechanics, pp. 191–212, 1964.

Dybbs, A., and B. Ghorashi (eds). Laser Anemometry Advances and Applications 1991. New York: ASME, 1991.

Ergun, S. "Fluid Flow Through Packed Columns." Chemical Engineering Prog., vol. 48, pp. 89–94, 1952.

Forchheimer, P. "Wasserbewegung durch Boden." Z. VDI, vol. 45, pp. 1782–1788, 1901.

Gere, J. M., and S. P. Timoshenko. Mechanics of Materials. Third edition, PWS-Kent, 1990.

International Standards Organization. "Measurement of Fluid Flow by Means of Orifice Plates, Nozzles and Venturi Tubes Inserted in Circular Cross Section Conduits Running Full." ISO Standard 5167, Geneva, 1980.

Jones, D. P., and H. Krier. "Gas Flow Resistance Measurements Through Packed Beds at High Reynolds Numbers." ASME, J. Fluids Eng., vol. 105, pp. 168–173, 1983.

Kinghorn, F. C. "Flow Measurement in Swirling or Asymmetric Flow: A Review." Flow-Con 77 Proceedings, Institute of Measurement and Control, Gatton and Kent, U.K., 1977.

Kinghorn, F. C., A. Kennedy, and P. Bedin. "The Use of a Flow Straightener-Venturi-Nozzle Package in Swirling Flow." Report No. 618, National Engineering Laboratory, East Kilbride, Glasgow, Scotland, 1976.

Kreith, F., and O. K. Sonju. "The Decay of Turbulent Swirl in a Pipe." Journal of Fluid Mechanics, vol. 22, pp. 257–271, 1965.

Kuo, K. K., and C. C. Nydegger. "Flow Resistance Measurements and Correlation in Packed Beds of Gun Propellant." Journal of Ballistics, vol. 2, pp. 1–25, 1978.

Lugt, H. "Einfluss der Drallströmung auf die Durchflusszahlen genormter Drosselmessgeräte." Brennstoff-Warme-Kraft, vol. 13, pp. 121, 1963.

Miller, D. S. Internal Flow Systems. Second edition, BHRA Information Services Cranfield, 1990.

Miller, R. W. Flow Measurement Engineering Handbook. Second edition, New York: McGraw Hill, 1989.

Ower, E., and R. C. Pankhurst. The Measurement of Air Flow. Oxford: Pergamon Press, 1977.

Pichot, P. Compressor Application Engineering. Vol. 1, Houston: Gulf Publishing Company, 1986.

Robbins, R., and P. S. Gough. "Experimental Determination of Flow Resistance in Packed Beds of Gun Propellant." Proceedings of the 15th JANNAF Combustion Meeting, Chemical Propulsion Information Agency, Publication 297, 1978.

Sprenkle, R. E., and N. S. Courtright. "Straightening Vanes for Flow Measurement." Mechanical Engineering, vol. 80, pp. 71–73, 92–95, 1958.

Union Carbide. "Optical Properties and Application of Linde Cz Sapphire." Crystal Products Technical Bulletin, Industrial Chemicals Division, 1988.

Ward-Smith, A. J. Internal Fluid Flow. Oxford: Clarendon Press, 1980.

Wieghart, C. E. G. "On the Resistance of Screens." Aero. Quarterly, vol. 4, p. 186, 1953.

Whitaker, J., P. G. Bean, and E. Hay. "Measurement of Losses Across Multi-cell Flow Straightener." Report No. 461, National Engineering Laboratory, East Kilbride, Glasgow, Scotland, 1970.

Wilcox, S. F., and H. Krier. "Gas Flow Resistance Measurement Through Packed Beds At High Reynolds Number." Technical Report AAE 80-1, University of Illinois Aero and Astronautical Engineering Department, 1980.

Zanker, K. J. "The Development of a Flow Straightener For Use With Orifice-Plate Flow Meter in Disturbed Flows." Proceedings of the Symposium on Flow Measurement in Closed Conduits, vol. 2, pp. 395–415, HMSO, Edinburgh, 1962.

Zoltani, C. K. "Flow Resistance in Packed and Fluidized Beds: An Assessment of Current Practice." Proceedings of the 28th JANNAF Combustion Meeting, vol. I, Chemical Propulsion Information Agency Publication 573, Columbia, MD, October 1991.

APPENDIX:

THE BLOWDOWN PROCESS

INTENTIONALLY LEFT BLANK.

THE BLOWDOWN PROCESS

A mass M of gas is contained in a tank of volume V. Through an opening of area A the gas exits. Choked conditions prevail at the exit from time t = 0 to time t = t_f. It is desired to calculate the pressure history during the emptying process as well as the time needed from the initial opening of the valve to the time that choking conditions can no longer be maintained. It is assumed that the flow process is isentropic and k is the ratio of specific heats in the gas.

$$\frac{dM}{dt} = - \dot{m} \tag{A-1}$$

$$\rho = \frac{M}{V} = \rho_i \left(\frac{p}{p_i} \right)^{1/k} , \tag{A-2}$$

where i denotes the initial state. Differentiating the above expression,

$$\left(\frac{p}{p_i} \right)^{\frac{(1-k)}{k}} \frac{d\,(\rho/\rho_i)}{dt} = - \frac{k\dot{m}}{\rho_i V} = \frac{kGA}{\rho_i V} , \tag{A-3}$$

where the critical mass flux is given by

$$G_c / \left(k \rho_i p_i \right)^{0.5} = \left(\frac{2}{k+1} \right)^{\frac{k+1}{2(k-1)}} . \tag{A-4}$$

Note that the conditions in the reservoir are continuously changing and these time-dependent conditions have to be reflected in the use of Equation (A-4).

Substituting and rearranging,

$$\left(\frac{p}{p_i}\right)^{\frac{1-3k}{2k}} \frac{d\,(p/p_i)}{dt} = -\left(k\,A/(\rho_i V)\right)\sqrt{(k p_i\,\rho_i)}\left(\frac{2}{k+1}\right)^{\frac{k+1}{2(k-1)}}, \qquad \text{(A-5)}$$

this is a differential equation with the initial conditions,

$$\text{at } t = 0\,, \quad p/p_i = 1\,.$$

Let $(p/p_i) = x$ and let $n = (1 - 3k)/2k$. The equation then can be written in the simplified form as follows:

$$x^n \frac{dx}{dt} = C\,. \qquad \text{(A-6)}$$

Here C is a constant, the value being the right-hand side of Equation A-5. This is the classical Bernoulli equation. The substitution $v = x^{n+1}$ reduces it to a linear equation which was first solved by Leibniz in 1696. The result is

$$\left(\frac{p}{p_i}\right) = \left[1 + \left(\frac{k-1}{2}\right)\left(\frac{2}{k+1}\right)^{\frac{(k+1)}{2(k-1)}}\left(\sqrt{\frac{k\,p_i}{\rho_i}}\right)\frac{At}{V}\right]^{\frac{-2k}{(k-1)}}, \qquad \text{(A-7)}$$

which alternatively can be solved for t for a given (p/p_i) ratio.

LIST OF SYMBOLS

A	cross-sectional area
C_D	discharge coefficient
C_d	flow coefficient
D	bed (pipe) diameter
d	wire diameter, orifice diameter
d_p	particle diameter
F	drag force
f	friction factor
G	mass flow rate per unit area
g	acceleration due to gravity
h	hydraulic height
K	pressure drop coefficient
k	roughness, also ratio of specific heats
L	length
M	angular momentum flux, also total mass
m	number of wires per unit length, also ρQ
N	number of particles
p	pressure
Q	volume flow rate
Re	Reynolds number = $\frac{\rho U D}{\mu}$
t	plate thickness
U	mean approach flow velocity
V	volume
W	swirl parameter

GREEK

β	open area
ϵ	void fraction
λ	area ratio
μ	viscosity

ξ porosity of plate

ρ density

σ stress

τ shear stress

ϕ coefficient of contraction

SUBSCRIPT

ang angular

c critical condition (choked)

i initial value

m mean

p particle

v velocity

1 circumferential

2 orifice

∞ free stream condition

No. of Copies	Organization
2	Administrator Defense Technical Info Center ATTN: DTIC-DDA Cameron Station Alexandria, VA 22304-6145
1	Commander U.S. Army Materiel Command ATTN: AMCAM 5001 Eisenhower Ave. Alexandria, VA 22333-0001
1	Commander U.S. Army Laboratory Command ATTN: AMSLC-DL 2800 Powder Mill Rd. Adelphi, MD 20783-1145
2	Commander U.S. Army Armament Research, Development, and Engineering Center ATTN: SMCAR-IMI-I Picatinny Arsenal, NJ 07806-5000
2	Commander U.S. Army Armament Research, Development, and Engineering Center ATTN: SMCAR-TDC Picatinny Arsenal, NJ 07806-5000
1	Director Benet Weapons Laboratory U.S. Army Armament Research, Development, and Engineering Center ATTN: SMCAR-CCB-TL Watervliet, NY 12189-4050
(Unclass. only) 1	Commander U.S. Army Rock Island Arsenal ATTN: SMCRI-TL/Technical Library Rock Island, IL 61299-5000
1	Director U.S. Army Aviation Research and Technology Activity ATTN: SAVRT-R (Library) M/S 219-3 Ames Research Center Moffett Field, CA 94035-1000
1	Commander U.S. Army Missile Command ATTN: AMSMI-RD-CS-R (DOC) Redstone Arsenal, AL 35898-5010

No. of Copies	Organization
1	Commander U.S. Army Tank-Automotive Command ATTN: ASQNC-TAC-DIT (Technical Information Center) Warren, MI 48397-5000
1	Director U.S. Army TRADOC Analysis Command ATTN: ATRC-WSR White Sands Missile Range, NM 88002-5502
1	Commandant U.S. Army Field Artillery School ATTN: ATSF-CSI Ft. Sill, OK 73503-5000
(Class. only) 1	Commandant U.S. Army Infantry School ATTN: ATSH-CD (Security Mgr.) Fort Benning, GA 31905-5660
(Unclass. only) 1	Commandant U.S. Army Infantry School ATTN: ATSH-CD-CSO-OR Fort Benning, GA 31905-5660
1	WL/MNOI Eglin AFB, FL 32542-5000
	Aberdeen Proving Ground
2	Dir, USAMSAA ATTN: AMXSY-D AMXSY-MP, H. Cohen
1	Cdr, USATECOM ATTN: AMSTE-TC
3	Cdr, CRDEC, AMCCOM ATTN: SMCCR-RSP-A SMCCR-MU SMCCR-MSI
1	Dir, VLAMO ATTN: AMSLC-VL-D
10	Dir, USABRL ATTN: SLCBR-DD-T

No. of Copies	Organization
1	Commander U.S. Army Concepts Analysis Agency ATTN: D. Hardison 8120 Woodmont Ave. Bethesda, MD 20014
1	C.I.A. 01R/DB/Standard Washington, DC 20505
1	Director U.S. Army Ballistic Missile Defense Systems Command Advanced Technology Center P. O. Box 1500 Huntsville, AL 35807-3801
1	Chairman DOD Explosives Safety Board Room 856-C Hoffman Bldg. 1 2461 Eisenhower Ave. Alexandria, VA 22331-0600
1	Department of the Army Office of the Product Manager 155mm Howitzer, M109A6, Paladin ATTN: SFAE-AR-HIP-IP, Mr. R. De Kleine Picatinny Arsenal, NJ 07806-5000
2	Commander Production Base Modernization Agency U.S. Army Armament Research, Development, and Engineering Center ATTN: AMSMC-PBM, A. Siklosi AMSMC-PBM-E, L. Laibson Picatinny Arsenal, NJ 07806-5000
3	PEO-Armaments Project Manager Tank Main Armament Systems ATTN: AMCPM-TMA/K. Russell AMCPM-TMA-105 AMCPM-TMA-120, C. Roller Picatinny Arsenal, NJ 07806-5000

No. of Copies	Organization
15	Commander U.S. Army Armament Research, Development, and Engineering Center ATTN: SMCAR-AEE SMCAR-AEE-B, A. Beardell D. Downs S. Einstein S. Westley S. Bernstein J. Rutkowski B. Brodman R. Cirincione A. Grabowsky P. Hui J. O'Reilly P. O'Reilly N. DeVries SMCAR-AES, S. Kaplowitz, Bldg. 321 Picatinny Arsenal, NJ 07806-5000
2	Commander U.S. Army Armament Research, Development, and Engineering Center ATTN: SMCAR-CCD, D. Spring SMCAR-CCH-V, C. Mandala Picatinny Arsenal, NJ 07806-5000
1	Commander U.S. Army Armament Research, Development, and Engineering Center ATTN: SMCAR-HFM, E. Barrieres Picatinny Arsenal, NJ 07806-5000
1	Commander U.S. Army Armament Research, Development, and Engineering Center ATTN: SMCAR-FSA-T, M. Salsbury Picatinny Arsenal, NJ 07806-5000
1	Commander, USACECOM R&D Technical Library ATTN: ASQNC-ELC-IS-L-R, Myer Center Fort Monmouth, NJ 07703-5301

No. of Copies	Organization
1	Commander U.S. Army Harry Diamond Laboratories ATTN: SLCHD-TA-L 2800 Powder Mill Rd. Adelphi, MD 20783-1145
1	Commandant U.S. Army Aviation School ATTN: Aviation Agency Fort Rucker, AL 36360
2	Program Manager U.S. Army Tank-Automotive Command ATTN: AMCPM-ABMS, T. Dean (2 cps) Warren, MI 48092-2498
1	Program Manager U.S. Army Tank-Automotive Command Fighting Vehicles Systems ATTN: SFAE-ASM-BV Warren, MI 48092-2498
1	Project Manager Abrams Tank System ATTN: SFAE-ASM-AB Warren, MI 48397-5000
1	Director HQ, TRAC RPD ATTN: ATCD-MA Fort Monroe, VA 23651-5143
2	Director U.S. Army Materials Technology Laboratory ATTN: SLCMT-ATL (2 cps) Watertown, MA 02172-0001
1	Commander U.S. Army Research Office ATTN: Technical Library P.O. Box 12211 Research Triangle Park, NC 27709-2211
1	Commander U.S. Army Belvoir Research and Development Center ATTN: STRBE-WC Fort Belvoir, VA 22060-5006

No. of Copies	Organization
1	Director U.S. Army TRAC-Ft. Lee ATTN: ATRC-L, Mr. Cameron Fort Lee, VA 23801-6140
1	Commandant U.S. Army Command and General Staff College Fort Leavenworth, KS 66027
1	Commandant U.S. Army Special Warfare School ATTN: Rev and Trng Lit Div Fort Bragg, NC 28307
3	Commander Radford Army Ammunition Plant ATTN: SMCAR-QA/HI LIB (3 cps) Radford, VA 24141-0298
1	Commander U.S. Army Foreign Science and Technology Center ATTN: AMXST-MC-3 220 Seventh Street, NE Charlottesville, VA 22901-5396
2	Commander Naval Sea Systems Command ATTN: SEA 62R SEA 64 Washington, DC 20362-5101
1	Commander Naval Air Systems Command ATTN: AIR-954-Technical Library Washington, DC 20360
1	Naval Research Laboratory Technical Library Washington, DC 20375
2	Commandant U.S. Army Field Artillery Center and School ATTN: ATSF-CO-MW, E. Dublisky (2 cps) Fort Sill, OK 73503-5600

No. of Copies	Organization
1	Office of Naval Research ATTN: Code 473, R. S. Miller 800 N. Quincy Street Arlington, VA 22217-9999
3	Commandant U.S. Army Armor School ATTN: ATZK-CD-MS, M. Falkovitch (3 cps) Armor Agency Fort Knox, KY 40121-5215
2	Commander U.S. Naval Surface Warfare Center ATTN: J. P. Consaga C. Gotzmer Indian Head, MD 20640-5000
4	Commander Naval Surface Warfare Center ATTN: Code 730 Code R-13, K. Kim R. Bernecker H. Sandusky Silver Spring, MD 20903-5000
2	Commanding Officer Naval Underwater Systems Center ATTN: Code 5B331, R. S. Lazar Technical Library Newport, RI 02840
1	Director Benet Weapons Laboratories ATTN: SMCAR-CCB-RA, G. P. O'Hara Watervliet, NY 12189-4050
4	Commander Dahlgren Division Naval Surface Warfare Center ATTN: Code G30, Guns and Munitions Division Code G301, D. Wilson Code G32, Gun Systems Branch Code E23, Technical Library Dahlgren, VA 22448-5000

No. of Copies	Organization
3	Commander Naval Weapons Center ATTN: Code 388, C. F. Price Code 3895, T. Parr Information Science Division China Lake, CA 93555-6001
1	OSD/SDIO/IST ATTN: Dr. Len Caveny Pentagon Washington, DC 20301-7100
4	Commander Indian Head Division Naval Surface Warfare Center ATTN: Code 610, T. C. Smith D. Brooks K. Rice Technical Library Indian Head, MD 20640-5035
1	OLAC PL/TSTL ATTN: D. Shiplett Edwards AFB, CA 93523-5000
1	AFATL/DLYV Eglin AFB, FL 32542-5000
1	AFATL/DLXP Eglin AFB, FL 32542-5000
1	AFATL/DLJE Eglin AFB, FL 32542-5000
1	AFELM, The Rand Corporation ATTN: Library D 1700 Main Street Santa Monica, CA 90401-3297
3	AAI Corporation ATTN: J. Hebert J. Frankle D. Cleveland P.O. Box 126 Hunt Valley, MD 21030-0126

No. of Copies	Organization
3	AL/LSCF ATTN: J. Levine L. Quinn T. Edwards Edwards AFB, CA 93523-5000
1	AVCO Everett Research Laboratory ATTN: D. Stickler 2385 Revere Beach Parkway Everett, MA 02149-5936
1	General Electric Company Tactical Systems Department ATTN: J. Mandzy 100 Plastics Ave. Pittsfield, MA 01201-3698
1	IITRI ATTN: M. J. Klein 10 W. 35th Street Chicago, IL 60616-3799
1	Hercules, Inc. Allegheny Ballistics Laboratory ATTN: William B. Walkup P.O. Box 210 Rocket Center, WV 26726
1	Hercules, Inc. Radford Army Ammunition Plant ATTN: E. Hibshman Radford, VA 24141-0299
1	Hercules, Inc. Hercules Plaza ATTN: B. M. Riggleman Wilmington, DE 19894
3	Director Lawrence Livermore National Laboratory ATTN: L-355, A. Buckingham M. Finger L-324, M. Constantino P.O. Box 808 Livermore, CA 94550-0622

No. of Copies	Organization
1	Olin Corporation Badger Army Ammunition Plant ATTN: F. E. Wolf Baraboo, WI 53913
3	Olin Ordnance ATTN: E. J. Kirschke A. F. Gonzalez D. W. Worthington P.O. Box 222 St. Marks, FL 32355-0222
1	Olin Ordnance ATTN: H. A. McElroy 10101 9th Street, North St. Petersburg, FL 33716
1	Paul Gough Associates, Inc. ATTN: Dr. Paul S. Gough 1048 South Street Portsmouth, NH 03801-5423
1	Physics International Company ATTN: Library, H. Wayne Wampler 2700 Merced Street San Leandro, CA 98457-5602
1	Princeton Combustion Research Laboratory, Inc. ATTN: M. Summerfield 475 U.S. Highway One Monmouth Junction, NJ 08852-9650
2	Rockwell International Rocketdyne Division ATTN: BA08, J.E. Flanagan J. Gray 6633 Canoga Ave. Canoga Park, CA 91303-2703
1	Sverdrup Technology, Inc. ATTN: Dr. John Deur 2001 Aerospace Parkway Brook Park, OH 44142

No. of Copies	Organization
2	Thiokol Corporation Elkton Division ATTN: R. Biddle Technical Library P.O. Box 241 Elkton, MD 21921-0241
1	Veritay Technology, Inc. ATTN: E. Fisher 4845 Millersport Highway East Amherst, NY 14501-0305
1	Universal Propulsion Company ATTN: H. J. McSpadden 25401 North Central Ave. Phoenix, AZ 85027-7837
1	Battelle ATTN: TACTEC Library, J.N. Huggins 505 King Ave. Columbus, OH 43201-2693
1	Brigham Young University Department of Chemical Engineering ATTN: M. Beckstead Provo, UT 84601
1	California Institute of Technology 204 Karman Laboratory Main Stop 301-46 ATTN: F.E.C. Culick 1201 E. California Street Pasadena, CA 91109
1	Jet Propulsion Laboratory California Institute of Technology ATTN: L. Strand, MS 125-224 4800 Oak Grove Drive Pasadena, CA 91109-8099
1	University of Illinois Department of Mechanical/Industrial Engineering ATTN: H. Krier 144 MEB; 1206 N. Green Street Urbana, IL 61801-2978

No. of Copies	Organization
1	University of Massachusetts Department of Mechanical Engineering ATTN: K. Jakus Amherst, MA 01002-0014
1	University of Minnesota Department of Mechanical Engineering ATTN: E. Fletcher Minneapolis, MN 55414-3368
3	Georgia Institute of Technology School of Aerospace Engineering ATTN: B.T. Zim E. Price W.C. Strahle Atlanta, GA 30332
1	Institute of Gas Technology ATTN: D. Gidaspow 3424 S. State Street Chicago, IL 60616-3896
1	Johns Hopkins University Applied Physics Laboratory Chemical Propulsion Information Agency ATTN: T. Christian Johns Hopkins Road Laurel, MD 20707-0690
1	Massachusetts Institute of Technology Department of Mechanical Engineering ATTN: T. Toong 77 Massachusetts Ave. Cambridge, MA 02139-4307
1	Pennsylvania State University Department of Mechanical Engineering ATTN: V. Yang University Park, PA 16802-7501
1	Pennsylvania State University Department of Mechanical Engineering ATTN: K. Kuo University Park, PA 16802-7501

No. of Copies	Organization
1	Pennsylvania State University Assistant Professor Department of Mechanical Engineering ATTN: Dr. Stefan T. Thynell 219 Hallowell Building University Park, PA 16802-7501
1	Pennsylvania State University Director, Gas Dynamics Laboratory Department of Mechanical Engineering ATTN: Dr. Gary S. Settles 303 Mechanical Engineering Building University Park, PA 16802-7501
1	SRI International Propulsion Sciences Division ATTN: Technical Library 333 Ravenwood Ave. Menlo Park, CA 94025-3493
1	Rensselaer Polytechnic Institute Department of Mathematics Troy, NY 12181
2	Director Los Alamos Scientific Laboratory ATTN: T3, D. Butler M. Division, B. Craig P.O. Box 1663 Los Alamos, NM 87544
1	General Applied Sciences Laboratory ATTN: J. Erdos 77 Raynor Ave. Ronkonkama, NY 11779-6649
1	Battelle PNL ATTN: Mr. Mark Garnich P.O. Box 999 Richland, WA 99352
1	Stevens Institute of Technology Davidson Laboratory ATTN: R. McAlevy III Castle Point Station Hoboken, NJ 07030-5907

No. of Copies	Organization
1	Rutgers University Department of Mechanical and Aerospace Engineering ATTN: S. Temkin University Heights Campus New Brunswick, NJ 08903
1	University of Southern California Mechanical Engineering Department ATTN: 0HE200, M. Gerstein Los Angeles, CA 90089-5199
1	University of Utah Department of Chemical Engineering ATTN: A. Baer Salt Lake City, UT 84112-1194
1	Washington State University Department of Mechanical Engineering ATTN: C. T. Crowe Pullman, WA 99163-5201
1	Alliant Techsystems, Inc. ATTN: R. E. Tompkins MN38-3300 5700 Smetana Drive Minnetonka, MN 55343
1	Alliant Techsystems, Inc. ATTN: J. Kennedy 7225 Northland Drive Brooklyn Park, MN 55428
1	Science Applications, Inc. ATTN: R. B. Edelman 23146 Cumorah Crest Drive Woodland Hills, CA 91364-3710
1	Battelle Columbus Laboratories ATTN: Mr. Victor Levin 505 King Ave. Columbus, OH 43201-2693
1	Allegheny Ballistics Laboratory Propulsion Technology Department Hercules Aerospace Company ATTN: Mr. Thomas F. Farabaugh P.O. Box 210 Rocket Center, WV 26726

No. of
Copies Organization

1 MBR Research Inc.
ATTN: Dr. Moshe Ben-Reuven
601 Ewing St., Suite C-22
Princeton, NJ 08540

Aberdeen Proving Ground

1 Cdr, USACSTA
ATTN: STECS-PO, R. Hendricksen

USER EVALUATION SHEET/CHANGE OF ADDRESS

This Laboratory undertakes a continuing effort to improve the quality of the reports it publishes. Your comments/answers to the items/questions below will aid us in our efforts.

1. BRL Report Number BRL-MR-3992 Date of Report July 1992

2. Date Report Received _____

3. Does this report satisfy a need? (Comment on purpose, related project, or other area of interest for which the report will be used.) _____

4. Specifically, how is the report being used? (Information source, design data, procedure, source of ideas, etc.) _____

5. Has the information in this report led to any quantitative savings as far as man-hours or dollars saved, operating costs avoided, or efficiencies achieved, etc? If so, please elaborate. _____

6. General Comments. What do you think should be changed to improve future reports? (Indicate changes to organization, technical content, format, etc.) _____

CURRENT ADDRESS

Name

Organization

Address

City, State, Zip Code

7. If indicating a Change of Address or Address Correction, please provide the New or Correct Address in Block 6 above and the Old or Incorrect address below.

OLD ADDRESS

Name

Organization

Address

City, State, Zip Code

(Remove this sheet, fold as indicated, staple or tape closed, and mail.)

DEPARTMENT OF THE ARMY
Director
U.S. Army Ballistic Research Laboratory
ATTN: SLCBR-DD-T
Aberdeen Proving Ground, MD 21005-5066

OFFICIAL BUSINESS

BUSINESS REPLY MAIL
FIRST CLASS PERMIT No 0001, APG, MD

Postage will be paid by addressee.

Director
U.S. Army Ballistic Research Laboratory
ATTN: SLCBR-DD-T
Aberdeen Proving Ground, MD 21005-5066

NO POSTAGE
NECESSARY
IF MAILED
IN THE
UNITED STATES